Effect of the anisotropy of the cells on the topological properties of two- and three-dimensional froths

Patrick Richard, Jean-Paul Troadec, and Luc Oger*
Groupe Matière Condensée et Matériaux, UMR CNRS 6626, Université de Rennes I, 35042 Rennes Cedex, France

Annie Gervois
Service de Physique Théorique, Direction des Sciences de la Matière, CEA/Saclay, 91191 Gif-sur-Yvette Cedex, France
(Received 14 February 2001; published 25 May 2001)

We study the effect of the anisotropy of the cells on the topological properties of monodisperse two- and three-dimensional (3D) froths. These froths are built by Voronoï tessellation of actual assemblies of monosize disks (2D) and of many numerical packings of monosize disks (2D) and spheres (3D). We show that some topological properties of these froths can be simply related to the anisotropy of the cells.

DOI: 10.1103/PhysRevE.63.062401 PACS number(s): 82.70.Rr, 87.80.Pa, 61.43.Bn

The physics of disordered froths is of great interest because of their importance in metallurgy (grain aggregates), biology (cells), geology (fracture patterns), etc. Such structures can be represented in a simplified way by convex polyhedra filling space [three-dimensional (3D) froths] or by convex polygons covering the plane (2D froths), and it is well known that the statistical properties of the cells verify some ''universal'' empirical laws, namely Aboav's, Lewis's, or Lemaitre's laws [1–3].

More recently, it appeared that unconsolidated granular media may be modeled in a first step by packings of equal hard spheres [4,5] or disks [3] and that the local environment is well described with the help of their Voronoi tessellation. It has been shown that these artificial froths behave, from a topological and a metric point of view, like natural froths [5]. These assemblies, therefore, may be used as investigative tools for more general purposes. In this paper, we present results on the correlation between the anisotropy of the cells and the topological properties of monodisperse 2D and 3D froths issued from monosize packings of disks and spheres.

Packings of spheres are built numerically using five algorithms that have already been described in previous papers, as mentioned later. Here we just recall briefly their principles in three dimensions. They can be divided into three classes.

(i) Sequential algorithms. For these algorithms, the particles are placed one at a time. The simplest algorithm of this class is the random sequential adsorption (RSA) [6,7]. Spheres are deposited at random positions; if the last deposited particle overlaps any of those already present, it is removed, otherwise it is permanently fixed. We also use the modified random sequential adsorption algorithm [8] (MRSA). This algorithm, based on the RSA, allows particles overlapping one or several particles already present to make small displacements to eliminate these overlaps.

The next two sequential algorithms build packings under the influence of a directional force such as the gravity. The first one, the Visscher and Bolsterli algorithm [9], consists in launching randomly particles at the top of the box that contains the packing. A particle is definitively deposited when it is in a stable position, i.e., in contact with three particles already placed. The second one is Powell's algorithm [10], which is very similar to the previous one. It consists in adding spheres, at the lowest position, in contact with three randomly chosen spheres already placed.

(ii) Cooperative algorithms. We use the Jullien algorithm [4], which is based on the Jodrey-Tory construction [11]. It consists of slowly reducing overlaps of packing of growing soft spheres.

(iii) Dynamic algorithms. The last algorithm we use is a classical hard-sphere molecular-dynamics algorithm (event-driven) [12].

According to these algorithms, we can build packings of any packing fraction, C, between 0 and 0.74 (fcc packing fraction). The packings are made of approximately 16 000 spheres.

For the packings of disks, we use 2D versions of the algorithms mentioned above. The packings of disks can then have any packing fraction between 0 and 0.907 (triangular lattice). The numerical packings contain approximately 10 000 disks. We also use actual packings of disks built on an air table [13]. Such packings are then studied by numerical image analysis. The statistics are made on approximately 3000 disks.

Now, we build our froths and for that purpose we focus on the Voronoï tessellation of packings of monosize disks and of packings of monosize spheres. We recall that a Voronoï cell is defined as the ensemble of points closer to a given sphere (or disk) than to any other and is characteristic of the local environment around this particle. We have represented in Fig. 1 an example of a Voronoï tessellation of a packing of disks.

In 2D, the topological properties of a cell are linked to its number of edges n. Due to Euler's relation, the mean value of edges per cell, $\langle n \rangle$, is a constant equal to 6. Thus, the topological energy of a 2D froth can be defined as the variance of n: $\mu_2(n) = \langle n^2 \rangle - \langle n \rangle^2$. Metric characteristics of such 2D froths are the mean area $\langle a \rangle$, the mean perimeter of the cells $\langle l \rangle$, and any higher moments of these quantities.

For 3D froths, things are a little more complicated. As the mean number of faces $\langle f \rangle$ is not a constant [5], we have to

*Electronic address: luc.oger@univ-rennes1.fr

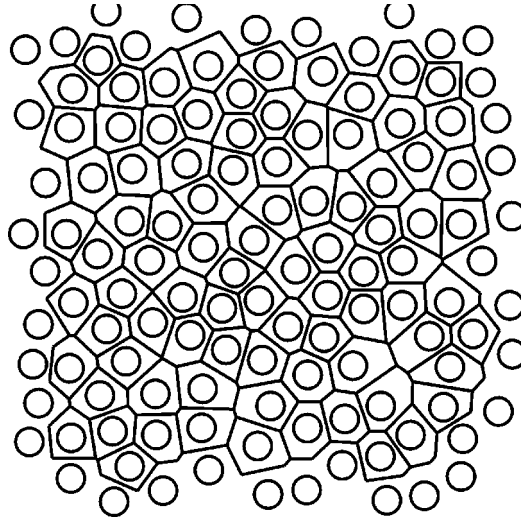

FIG. 1. Example of a 2D Voronoï tessellation. Each cell is a convex polygon. The set of cells fills the plane.

consider both this mean number and the variance of f, $\mu_2(f)=\langle f^2\rangle-\langle f\rangle^2$. As for 2D froths, we can compute the mean volume $\langle V\rangle$, area $\langle A\rangle$, and perimeter $\langle L\rangle$ of the cells and any higher moment of these quantities.

We have plotted in Fig. 2 the evolution of $\langle f\rangle$ versus the packing fraction for the different algorithms used. We observe that this quantity depends not only on the packing fraction but also on the algorithm used, i.e., on the history of the packing. So the packing fraction is clearly not a good quantity in order to describe the state of a froth, and we now look for a better parameter. We can turn to the relation between $\langle f\rangle$ and the anisotropy of the cells. This can be done qualitatively by looking at Fig. 2. First, we can compare the different algorithms for a given packing fraction. Second, for a given algorithm (for which we can modify the packing fraction), we observe a decrease of $\langle f\rangle$ when the packing fraction increases; actually, it may be checked that cells become more isotropic with this increase.

For example, due to its principle of construction, the MRSA algorithm provides very distorted cells. The Visscher-Bolsterli and Powell algorithms also give anisotropic cells since the direction of the gravity is favored. The last example is the event-driven algorithm: for high packing fractions ($C>0.545$), the system crystallizes [12]; the cells are then more isotropic than those of disordered packings at the same packing fraction. We observe in Fig. 2 that the higher the anisotropy, the higher the value of $\langle f\rangle$. This result is in agreement with a theory developed by Rivier [14], who

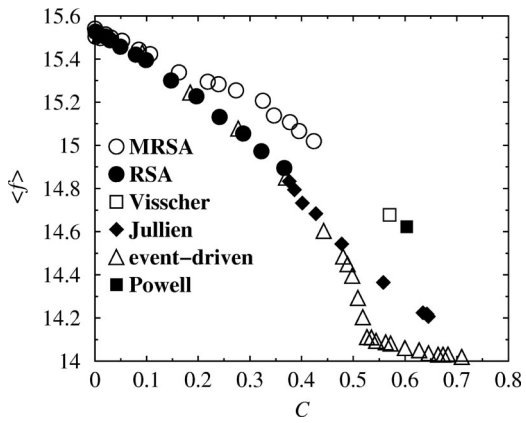

FIG. 2. Evolution of the mean number of faces versus the packing fraction, C, for different algorithms.

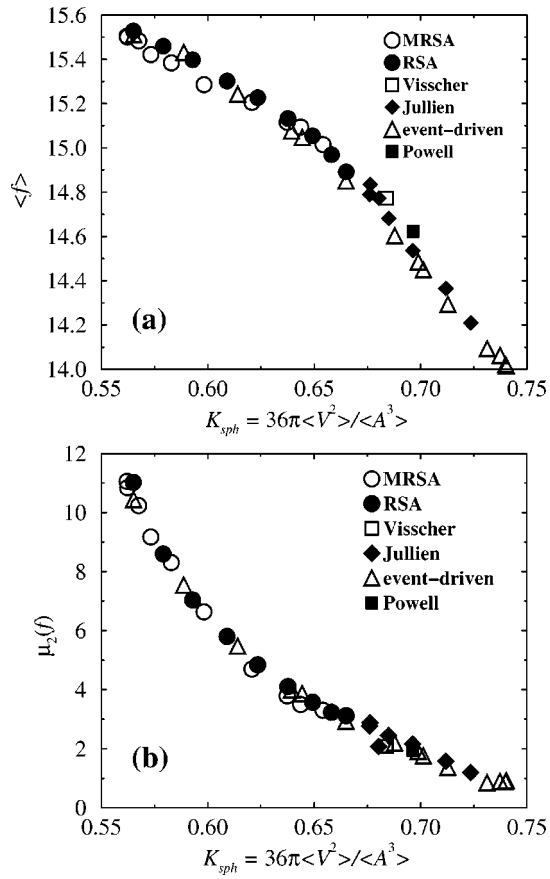

FIG. 3. Evolution of the mean number of faces (a) and of the variance of the number of faces (b) versus the sphericity coefficient K_{sph} for all the algorithms used.

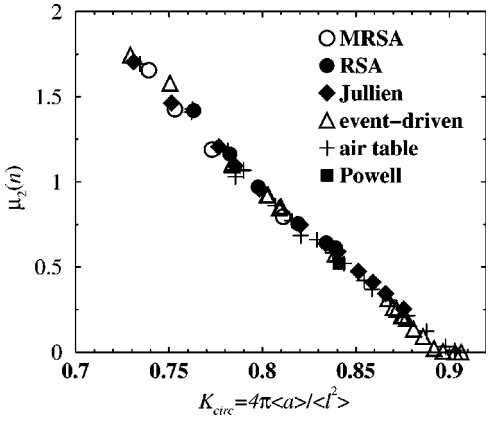

FIG. 4. Evolution of the variance of the number of edges of the cells versus the coefficient K_{circ}, for froths generated from 2D disk packings.

has shown that fluctuations in the average curvature imparted by each vertex of a cell lead to an increase of $\langle f \rangle$.

In order to describe more quantitatively the anisotropy of the cells, we have computed for each packing a sphericity coefficient of the cells, which we define by

$$K_{\mathrm{sph}} = 36\pi \langle V^2 \rangle / \langle A^3 \rangle. \quad (1)$$

For a sphere, this coefficient is equal to 1. For a convex polyhedron, the more anisotropic the polyhedron, the lower is K_{sph}. We have reported in Fig. 3(a) the variation of $\langle f \rangle$ versus this coefficient. In agreement with Rivier's theory and with our previous qualitative study, we find that the higher the anisotropy, the higher is $\langle f \rangle$. Furthermore, surprisingly, it seems that all points are positioned on a unique curve. We have also represented, in Fig. 3(b), the evolution of the variance of f, $\mu_2(f)$, with the sphericity coefficient, and we find once more a unique curve for all the algorithms used. So, unlike the packing fraction (see Fig. 2), the sphericity coefficient seems to be a good parameter in order to describe the 3D froths: all the algorithms used give similar results for a given anisotropy.

Then, we checked whether a similar law can be found for 2D froths. We first define the 2D equivalent of the sphericity coefficient for 2D froths,

$$K_{\mathrm{circ}} = 4\pi \langle a \rangle / \langle l^2 \rangle. \quad (2)$$

We have reported in Fig. 4 the evolution of $\mu_2(n)$ for all packings of disks used versus the coefficient K_{circ}. All the points seem to be in the same curve. As in 3D, the different froths give similar results for a given anisotropy. We can also notice that this curve is linear except on a very short range of packing fraction, where the packings of disks are crystallized ($C > 0.89$) and $\mu_2(n) \approx 0$.

In conclusion, in this Brief Report we have reported studies on the effect of the anisotropy of cells of disordered 2D and 3D froths on their topological properties. In order to build our froths, we use the Voronoï tessellation of packings of monosize particles built by numerical simulation. For the 2D froths, we also use actual packings built on an air table. For 3D froths, we have shown, in agreement with Rivier's theory, that the mean number of faces $\langle f \rangle$ increases when the anisotropy of the cells increases. A more careful study shows that this quantity and the variance of the number of faces $\mu_2(f)$ seem to depend universally on this anisotropy. A similar result exists in 2D.

It remains to check whether that universality is verified by natural froths such as, for example, polycrystals. The answer is difficult because it is not easy to measure the mean quantities in the expression of K_{sph}. The next step of this work is to study the link between the anisotropy of the 3D froths and the anisotropy of their cuts (see [15] for a preliminary work on cuts of 3D froths). We expect to find information on the 3D structure from the cuts.

[1] D. Aboav, Metallography **3**, 383 (1970).
[2] F. Lewis, Anat. Rec. **38**, 341 (1928).
[3] J. Lemaître, A. Gervois, J.-P. Troadec, N. Rivier, M. Ammi, L. Oger, and D. Bideau, Philos. Mag. B **67**, 347 (1993).
[4] R. Jullien, P. Jund, D. Caprion, and D. Quitmann, Phys. Rev. E **54**, 6035 (1996).
[5] L. Oger, A. Gervois, J.-P. Troadec, and N. Rivier, Philos. Mag. B **47**, 177 (1996).
[6] B. Widom, J. Chem. Phys. **4**, 3888 (1966).
[7] E. L. Hinrichsen, J. Feder, and T. Jossang, J. Stat. Phys. **44**, 793 (1986).
[8] R. Jullien and P. Meakin, J. Phys. A **25**, L189 (1992).
[9] W. Visscher and M. Bolsterli, Nature (London) **239**, 504 (1972).
[10] M. Powell, Powder Technol. **25**, 45 (1980).
[11] W. Jodrey and E. Tory, Phys. Rev. A **32**, 2347 (1985).
[12] P. Richard, L. Oger, J.-P. Troadec, and A. Gervois, Phys. Rev. E **60**, 4551 (1999).
[13] J. Lemaître, A. Gervois, H. Peerhossaini, D. Bideau, and J.-P. Troadec, J. Phys. D **23**, 1396 (1990).
[14] N. Rivier, J. Phys. (Paris), Colloq. **C9**, 91 (1982).
[15] L. Oger, P. Richard, J.-P. Troadec, and A. Gervois, Eur. Phys. J. B **14**, 403 (2000).